Two-dimensional metal coordination networks hydrothermal synthesis, crystal structure, and thermal properties of $^{2}_{\infty}$[M(ox)(bpy)] (M = Fe, Co, Ni, Zn; ox = $C_2O_4^{2-}$; bpy = 4, 4'-bipyridine) and $^{2}_{\infty}$[MCl_2(bpy)] (M = Fe, Co, Ni, Co/Ni)

Michael A. Lawandy*, Xiaoying Huang, Jack Y. Lu, Ru-Ji Wang, and Jing Li
Department of Chemistry, Rutgers University, Camden, New Jersey, 08102

*Rutgers Undergraduate Research Fellow

Abstract

Two-dimensional metal coordination polymers with a general formula $^{2}_{\infty}$[M(ox)(bpy)] (M = Fe, Co, Ni, Zn; ox = $C_2O_4^{2-}$; bpy = 4, 4'-bipyridine) and [MCl_2(bpy)] (M = Fe, Co, Ni, or Co/Ni; 1:1 molar) bpy = 4, 4'-bipyridine) have been designed and synthesized via the hydrothermal method. The compounds $^{2}_{\infty}$[Fe(ox)(bpy)](**I**), $^{2}_{\infty}$[Co(ox)(bpy)](**II**), $^{2}_{\infty}$[Ni(ox)(bpy)](**III**), and $^{2}_{\infty}$[Zn(ox)(bpy)](**IV**) represent the first coordination network structure constructed by bridging oxalate and 4,4'-bpy mixed ligands. The compounds $^{2}_{\infty}$[$FeCl_2$(bpy)](**V**), $^{2}_{\infty}$[$CoCl_2$(bpy)](**VI**), $^{2}_{\infty}$[$NiCl_2$(bpy)](**VII**), and $^{2}_{\infty}$[$ZnCl_2$(bpy)](**VIII**) represent a similar structure type constructed by bridging chlorine atoms and 4,4'-bpy ligands. Compounds I-IV are isostructural and belong to the orthorhombic crystal system, space group Immm (No. 71). Compounds **V**-**VIII** are also isostructural and belong to the orthorombic crystal system, space group Cmmm (No. 65). **I**-**IV** have a non-interpenetrated structure that contains layers of octahedral metal centers coordinated by two oxalate and two bpy ligands. In like fashion, **V**-**VIII** have a non-interpenetrated structure containing metal centers octahedrally coordinated to four bridging chlorine atoms and two bpy ligands at trans position. Thermogravimetric analyses (TGA) indicate that compounds **I**-**IV** are thermally stable up to 300°C, while compounds **V**-**VIII** are thermally stable up to 400°C.

Introduction

The hydrothermal method[1] has proven to be a very effective way to grow crystals and hence, has been widely used in the synthesis of various solid-state inorganic materials. The purpose of this study is to design and synthesize coordination polymers containing metal centers and rigid ligands via this technique[2]. Two ligands that have been selected are 4,4'-bipyridine and oxalate. The former ligand (bpy) is unique in its ability to act as a rigid, rod-like organic building block[3-9]. Oxalate is selected because of its strength, rigidity, and specificity. We describe the preparation, crystal structure analysis, and thermal properties of two new two-dimensional

coordination frameworks [M(ox)(bpy)] (M = Fe, Co, Ni, Zn; ox = $C_2O_4^{2-}$; bpy = 4, 4'-bipyridine) and [MCl_2(bpy)] (M = Fe, Co, Ni, Co/Ni).

Experimental Methods

Reagents

All chemicals used are as purchased without purification. $FeCl_2$ (99.5%, Alfa Aear), $FeBr_2$•$6H_2O$ (99.5%, Alfa Aesar), $FeCl_2$•$4H_2O$ (99+%, ACROS), $FeCl_3$ (98%, Strem), $CoCl_2$ (99.7%, Alfa Aesar), $CoCl_2$•$6H_2O$ (98%, ACROS), $CoBr_2$•$6H_2O$ (99%, Alfa Aesar), $NiCl_2$ (99%, Alfa Aesar), $NiCl_2$•$6H_2O$ (97%, ACROS), $NiBr_2$•$6H_2O$ (98%, Alfa Aesar), $ZnCl_2$ (98%, Aldrich), 4,4'-bypyridine (98%, Alfa Aesar), oxalic acid ($H_2C_2O_4$•$2H_2O$, 97%, Alfa Aesar), and sodium oxalate ($Na_2C_2O_4$, 99%, Alfa Aesar).

Synthesis of $^2_\infty$ [Fe(ox)(bpy)] (I)

The reactions of $FeBr_2$•$6H_2O$ (0.1618 g), bpy (0.0781 g), oxalic acid (0.063 g), and H_2O (4 mL) in the mole ratio of 1:1:1:444 in a 23 mL acid digestion bomb at 170^{o}C for a period of seven days resulted in red plate crystals of **I**. The product was washed with water and acetone and dried in air. Compound **I** was isolated in quantitative yield.

Synthesis of $^2_\infty$ [Co(ox)(bpy)] (II)

Orange plate crystals were isolated from the reaction of $CoBr_2$•$6H_2O$ (0.1638 g), bpy (0.0781 g), oxalate acid (0.0063 g), and H_2O (4 mL) in the mole ratio of 1:1:1:444. The reactions were carried out in a 23 mL acid digestion bomb at 170^{o}C for seven days. **II** in quantitative yield was collected. A single-phase polycrystalline sample of **II** was obtained in the reaction of $CoCl_2$ (0.1298 g), bpy (0.1562 g), sodium oxalate (0.1340 g) and H_2O (8 mL) in the molar ratio of 1:1:1:444 under the conditions described previously.

Synthesis of $^2_\infty$ [Ni(ox)(bpy)] (III)

The reaction of $NiBr_2$•$3H_2O$ (0.2665 g), bpy (0.1562 g), oxalate acid (0.1260 g), and H_2O (8 mL) in the mole ratio of 1:1:1:444 under the same conditions as described for crystal growth of **I** and **II** produced light blue plate crystals of **III** in quantitative yield. Similar reactions of $NiCl_2$ (0.1296 g), bpy (0.1562 g), sodium oxalate (0.1340 g), and H_2O (8 or16 mL) in the mole ratio of 1:1:1:444 or 888 yielded single phased powder samples of **III**.

Synthesis of $^2_\infty$ [Zn(ox)(bpy)] (IV)

Colorless transparent thin plate crystals of **IV** were grown from reactions of $ZnCl_2$ (0.0682 g), bpy (0.0781 g), oxalate acid (0.0630 g), and H_2O (8 mL) in the mole ratio of 1:1:1:888. The same reaction conditions were used as in the synthesis of compounds **I** and **II**. The yield for this reaction was approximately 60%. Subsequent reactions using $ZnCl_2$ (0.1363 g), bpy (0.1562 g), sodium oxalate (0.1340 g), and H_2O (8 mL) in the mole ratio of 1:1:1:444 under identical conditions yielded a polycrystalline, pure-phase samples of **IV**.

Synthesis of $^{2}_{\infty}$ [$FeCl_2$(bpy)] (V)

The reactions of $FeCl_3$ (0.1622 g), $H_2C_2O_4$•$2H_2O$ (0.1261 g), bpy (0.1562 g), and H_2O (5 mL) in the mole ratio of 1:1:1:278 under the previous conditions yielded brownish column-like crystals of **V**. The yield of this reaction was calculated to be 76%. Powder XRD analysis revealed that the mixing of $FeCl_2$•$4H_2O$ (0.1988 g) and bpy (0.1562 g) gave rise to Fe_2O_3. Only when $FeCl_3$ was used as the reagent in the presence of oxalic acid did single-phased V form.

Synthesis of $^{2}_{\infty}$ [$CoCl_2$(bpy)] (VI)

Pale pink-purple crystals were isolated from the reaction of $CoCl_{21}$•$6H_2O$ (0.1189 g), $H_2C_2O_4$•$2H_2O$ (0.063 g), bpy (0.0781 g), and H_2O (8 mL) in the mole ratio of 1:1:1:889 in a 23 mL acid digestion bomb at 170^{o}C for a period of seven days. The secondary product of this reaction was [Co(ox)(bpy)]. A single phased pale pink-purplish polycrystalline sample of **VI** was produced by subsequent reactions using $CoCl_2$ (0.1298 g) and bpy (0.1562g) in H_2O (8 mL) at 170^{o}C for 3 days. The yield for this reaction was 70%.

Synthesis of $^{2}_{\infty}$ [$NiCl_2$(bpy)] (VII)

Single-phased pale greenish-yellow polycrystalline samples of **VII** was produced from the the reaction of $NiCl_2$ (0.1296 g), bpy (0.1562 g), and H_2O (4 mL) in the mole ratio of 1:1:1:444 in a 23 mL acid digestion bomb at 170^{o}C for 3 days. The yield for this reaction was 72 %.

Synthesis of $^{2}_{\infty}$ [(Co/Ni)Cl_2(bpy)] (VIII)

The reaction of $CoCl_2$•$6H_2O$ (0.1190 g), $NiCl_2$•$6H_2O$ (0.1198 g), bpy (0.1562 g), and H_2O (8 mL) in the mole ratio of 1:1:1:444 in a 23 mL acid digestion bomb at 170^{o}C for 7 days yielded single-phased polycrystalline pale grayish samples of **VIII**. The yield for this reaction was 70%. The same product was obtained with anhydrous metal chlorides as reagents.

Crystallographic studies

A red plate crystal of **I** (0.2 x 0.3 x 0.5 mm), an orange plate crystal of **II** (0.1 x 0.2 x 0.5 mm), a light blue plate crystal of **III** (0.2 x 0.4 x 0.5 mm), a colorless plate crystal of **IV** (0.02 x 0.02 x 0.1 mm), a brownish blocklike crystal of **V** (0.06 x 0.08 x 0.13 mm), and a pale pink-purplish column-like crystal of **VI** were selected for the crystal structure analysis. Each crystal was mounted on a glass fiber in air on an Enraf-Nonius CAD4 automated diffractometer. Twenty-five reflections were centered in each case using graphite-monochromated Mo-Kα radiation. The data were collected at room temperature with w-scan method within the limits $7^o \leq 2\Theta \leq 50^o$ (**I-IV**), $5^o \leq 2\Theta \leq 52^o$ (**V**) and $7^o \leq 2\Theta \leq 50^o$ (**VI**). Raw data were corrected for Lorentz and polarization effects, and an empirical absorption correction[10] was applied in each case. The structures were solved using the SHELX-97 program[11]. The non-hydrogen atoms were located by direct phase determination and subjected to anisotropic refinement. The hydrogens were generated theoretically. The full-matrix least-square calculations on F2 were applied on the final refinements. The unit cell parameters, along with data collection and refinement details, are given in Table 1 and Table 6. Selected bond lengths and angles are reported in Tables 2-5 and Table 7. Crystal drawings were generated by SCHAKAL 92[12].

Attempts to grow crystals of **VII** and **VIII** suitable for structure analysis by single-crystal X-ray diffraction were not successful. The unit cells of these compounds were refined using powder XRD data of single-phased samples. The refinement was also performed on **V** and **VI** as a comparison. The refinement was performed using JADE (Windows) software package[13]. The refinement results, including those of **V** and **VI**, are listed in Table 8.

X-ray powder diffraction analyses were performed on a Rigaku D/M-2200T automated diffraction system (Ultima+). All measurements were made between a 2Θ range of 5^o and 80^o at the operating power of 40 kV/40 mA. All polycrystalline samples were examined for the purpose of phase identification.

Thermal analysis

Thermogravimetric (TGA) analyses of the title compounds were performed on a computer controlled TA Instrument 2050TGA analyzer. Single phased powder samples of **I** (9.4430 mg), **II** (5.4460 mg), **III** (11.0880), **IV** (28.1680 mg), **V** (23.424 mg), **VI** (20.832 mg), **VII** (13.369 mg), and **VIII** (19.686 mg) were loaded into alumina pans and heated with a ramp rate of 10^oC/min from room temperature to 500-550^{o}C for **I-IV** and to 800^{o}C for **V-VIII**.

Results and Discussion

Structures

Compounds **I-IV** crystallize in the orthorhombic crystal system, space group Immm (No. 71), while compounds **V-VIII** crystallize in the orthorombic crystal system, space group Cmmm (No. 65). The crystal structure of compounds **I-IV** consists of two-dimensional [M(ox)(bpy] networks (Figure 1) and the crystal structure of compounds **V-VIII** is similar to that of **I-IV**, also composed of two-dimensional networks (Figure 2). For compounds **I-IV**, the metal atoms are divalent and have an octahedral coordination with four oxygen atoms from oxalate ions and two nitrogen atoms from bipyridine molecules. Similarly, the metals are also divalent and have an octahedral coordination with four chloride atoms and by two nitrogen from bipyridine molecules in **V-VIII**. In all the compounds, the 2D sheets are formed in the *ac* plane by connecting metal centers via bridging chlorine (or oxalate) and 4,4'-bpy ligands. Hence, these compounds have rectangular-shaped voids that are enclosed by four M^{2+} located at the four corners of the rectangle, either two oxalates or four chlorine atoms, and two bpy's, each bridging to two metal centers (Figure 1.2). The approximate cross-section of these voids is 5 x 11 Å for **I-IV** and 3.6 x 11 Å for **V-VIII**. The 2D nets stack on top of each other at a distance of ½b to complete the structure in the third-dimension.

For compounds **I-IV**, all O-M-N and N-M-N angles are 90^o and 180^o, respectively. Likewise, for compounds **V-VIII**, all N-M-Cl and N-M-M angles are 90^o and 180^o, correspondingly. In compounds **I-IV**, the M-M distances within the 2D net are *a* (5.3-5.5Å) and *c* (11.3-11.5Å), respectively. Similarly, the M-M distances within the 2D net are *c* (3.58-3.62 Å) and *a* (11.33-11.41 Å). All bpy rings are perpendicular to the *ac* planes so that they are parallel to each other. The distance between any two adjacent rings is 3.3-3.5Å for compounds **I-IV** and 5.3-5.5Å for compounds **V-VIII**. These distances allows for weak π-π interactions, which often stabilizes the structures.

Thermal stability

Shown in Figures 3-8 are the results from thermogravimetric analyses (TGA) performed on **I**, **II**, **III**, **IV**, **V**, and **VI**. The curves of compounds **I-IV** indicate that these compounds underwent a single-step weight loss process and that they are thermally stable up to at least 300^{o}C. In addition, the curve for compound **V** indicates that this compound underwent a three-step weight loss process and that it is thermally stable to at least 400^{o}C. Also, the compounds **VI-VIII** underwent a two-step weight loss process and are at least stable to 400^{o}C. The decomposition process completed at approximately 450^{o}C for **I**, 475^{o}C for **II**, 525^{o}C for **III**, 425^{o}C for **IV**, and 800^{o}C for **V-VIII**. The thermal stability of these compounds may be attributed to the p-p interactions between the adjacent parallel bpy rings.

Conclusion

Two new types of two-dimensional coordination networks have been designed and synthesized via the hydrothermal method. Relatively high yields have been obtained for all compounds. The crystal structures have been analyzed by single crystal and powder XRD methods. Both [M(ox)(bpy)] and [MCl_2(bpy)] are quite stable due to the weak π-π interactions between the adjacent parallel bipyradine rings. Compounds **I-IV** are thermally stable up to 300^{o}C and compounds **V-VIII** are thermally stable up to 400^{o}C.

Acknowledgment

Financial support from the National Science Foundation (DMR-9553066) is greatly appreciated. The FT-IR/TGA/DSC apparatus was purchased through a NSF ARI grant (CHE 9601710-ARI).

References

(1) Ludise, R. A. In Progress in Inorganic Chemistry; Interscience Publishers: New York, 1962; Vol. III. Rabenau, A. Agnew. Chem. Int. Ed. Engl. **1985**, 24, 1026. Laudise, R. A., Chem. Eng. News **1987**, September 28, 30.

(2) See for example, Gutschke, S. O. H.; Slawin, A. M. Z.; Wood, P. T. J. Chem. Soc., Chem. Commun. **1995**, 2197. Yaghi, O. M.; Li, H. J. Am. Chem. Soc. **1996**, 117, 10401, Gutschke, S. O. H.; Molinier, M.; Powell, A. K.; Winpenny, E. P.; Wood, P. T. Chem. Commun. **1996**, 823. Yaghi, O. M.; Li, H. J. Am. Chem. Soc. **1996**, 118, 295.

(3) Gable, R. W.; Hoskins, B. F.; Robson, R. J. Chem. Soc., Chem. Commun. **1990**, 1677.

(4) Fujita, M.; Kwon, Y.; Washizu, S.; Ogura, K. J. Am. Chem. Soc. **1994**, 116, 1151.

(5) MacGillivray, L. R.; Subramanian, S.; Zaworotko, M. J. J. Chem. Soc., Chem. Commun. **1994**, 1325.

(6) Carlucci, L.; Ciani, G.; Proserpio, D. M.; Sironi, A. J. Chem. Soc., Chem. Commun. **1994**, 2755.

(7) Yaghi, O. M.; Li, G. Angew. Chem. Int. Ed. Engl. **1995**, 34, 207.

(8) Yaghi, O. M.; Li, H. J. Am. Chem. Soc. **1996**, 118, 295.

(9) Yaghi, O. M.; Li, H.; Groy, T. L. Inorg. Chem. **1997**, 36, 4292.

(10) Kopfmann, G.; Hubber, R. Acta Crystallogr. **1968**, A24, 348-351.

(11) Sheldrick, G.M. SHELX-97: program for structure refinement; University of Goettingen: Germany, **1997**.

(12) Keller, E. SCHAKAL 92: a computer program for the graphical representation of crystallographic models; University of Freiburg: Germany, **1992**.

(13) JADE for Windows: XRD Pattern Processing for the PC, 1991-1995 Materials Data, Inc.

Table 1. Cyrstallographic data for compounds I, II, III, and IV.

	I	**II**	**III**	**IV**
formula*	$^{2}_{\infty}$ [Fe(ox)(bpy)]	$^{2}_{\infty}$ [Co(ox)(bpy)]	$^{2}_{\infty}$ [Ni(ox)(bpy)]	$^{2}_{\infty}$ [$CoCl_2$(bpy)]
formula weight	300.05	303.13	302.91	309.57
space group	*Immm* (No. 71)	*Immm* (No. 71)	*Immm* (No. 71)	*Immm* (No. 71)
***a*, Å**	5.476(1)	5.385(2)	5.303(1)	5.378(1)
***b*, Å**	10.946(2)	10.945(2)	10.955(2)	10.967(2)
***c*, Å**	11.471(2)	11.374(1)	11.257(2)	11.443(2)
***V*, Å^3**	687.6(2)	670.4(2)	654.0(2)	674.9(2)
Z	2	2	2	2
ρ_{calc}, g cm^{-3}	1.449	1.502	1.538	1.523
μ, mm^{-1}	1.106	1.289	1.493	1.829
R [$I > 4\sigma(I)$]R_1[a]	0.044	0.026	0.024	0.040
***w*R_2**[b]	0.103	0.065	0.059	0.092

Notes to Table 1. *ox = C_2O_4; bpy = $N_2C_{10}H_8$.
[a]$2R_1 = \Sigma \mid |F_o| - |F_c| \mid / \Sigma \mid F_o|$
[b]$wR_2 = [\Sigma (F_o^2 - F_c^2)^2 / \Sigma w(F_o^4)]^{1/2}$
$w = [\sigma^2(F_o^2) + dP^2 + ep]^{-1}$; $P = (F_o^2 + 2F_c^2) / 3$
Values of *d* and *e* for **I**: 0.0, 55.02; for **II:** 0.0202, 0.91; for **III**: 0.0081, 0.60; for **IV**: 0.0402, 1.91.

Table 2. Bond Lengths [Å] and Angles [deg] for I.

Fe(1)-O(1)	2.116(4)	**Fe(1)-N(1)**	2.211(7)
O(1)-C(1)	1.237(6)		
O(1)-Fe(1)-O(1)	101.3(2)	**O(1)-Fe(1)-O(1)**	78.7(2)
O(1)-Fe(1)-O(1)	180.0	**O(1)-Fe(1)-N(1)**	90.0
N(1)-Fe(1)-N(1)	180.0		

Table 3. Bond Lengths [Å] and Angles [deg] for II.

Co(1)-O(1)	2.0767(18)	**Co(1)-N(1)**	2.147(3)
O(1)-C(1)	1.246(2)		
2O(1)-Co(1)-O(1)	180.0	**2O(1)-Co(1)-O(1)**	80.83(10)
2O(1)-Co(1)-O(1)	99.17(10)	**O(1)-Co(1)-N(1)**	90.0
N(1)- Co(1)- N(1)	180.0		

Table 4. Bond Lengths [Å] and Angles [deg] for III.

Ni(1)-O(1)	2.0477(18)	**Ni(1)-N(1)**	2.089(4)
O(1)-C(1)	1.246(2)		
2O(1)-Ni(1)-O(1)	97.63(9)	**2O(1)-Ni(1)-O(1)**	180.0
2O(1)-Ni(1)-O(1)	82.37(9)	**O(1)-Ni(1)-N(1)**	90.0
N(1)-Ni(1)-N(1)	180.0		

Table 5. Bond Lengths [Å] and Angles [deg] for IV.

Zn(1)-O(1)	2.083(3)	**Zn(1)-N(1)**	2.182(5)
O(1)-C(1)	1.245(4)		
2O(1)-Zn(1)-O(1)	180.0	**2O(1)-Zn(1)-O(1)**	81.28(16)
2O(1)-Zn(1)-O(1)	98.72(16)	**O(1)-Zn(1)-N(1)**	90.0
N(1)-Zn(1)-N(1)	180.0		

Table 6. Crystallographic Data for V and VI.

	V	VI
formula*	$^{2}_{\infty}$ [$FeCl_2$(bpy)]	$^{2}_{\infty}$ [$CoCl_2$(bpy)]
formula weight	282.93	286.01
space group	*Immm* (No. 65)	*Immm* (No. 65)
***a*, Å**	11.929(2)	11.993(2)
***b*, Å**	11.447(2)	11.374(2)
***c*, Å**	3.638(1)	3.611(1)
***V*, Å^3**	496.77(18)	492.57(18)
Z	2	2
ρ_{calc}, g cm^{-3}	1.891	1.928
μ, mm^{-1}	2.015	2.243
R [$I > 4\sigma(I)$]R_1[a]	0.044	0.026
***w*R_2[b]**	0.1136	0.1062
λ, Å	0.71073	0.71073

Notes to Table 1. Values of *d* and *e* for **V**: 0.0, 6.0; for **VI**: 0.0, 0.0. For other definitions, see Table 1.

Table 7. Selected Bond Lengths (Å) and Angles (deg) for V and VI.

	V		VI
Fe-N	2.184(9) 2×	**Co(1)-N(1)**	2.152(9) 2×
Fe-Cl	2.5042(17) 4×	**Co(1)-Cl(1)**	2.4869(19) 4×
N-C(1)	1.304(10) 2×	**N(1)-C(1)**	1.314(10) 2×
2O(1)-Co(1)-O(1)	99.17(10)	**O(1)-Co(1)-N(1)**	90.0
N-Fe-N	180.0	**N-Co-N**	180.0
N-Fe-Cl	90.0	**N-Co-Cl**	90.0
Cl-Fe-Cl	180.0,93.17(8),86.83(8)	**Cl-Co-Cl**	180.0,93.10(9),86.90(9)
Fe-Cl-Fe	93.17(8)	**Co-Cl-Co**	93.10(9)
C(1)-N-Fe	123.0(5)	**C(1)-N(1)-Co(1)**	122.7(5)

Table 8. Unit cell lengths (Å) for compounds V - VIII.

	v	**vI**	**vII**	**vIII**
a	11.945 (4)	11.954 (3)	11.972 (2)	11.928 (2)
b	11.455 (5)	11.411 (1)	11.332 (2)	11.352 (2)
c	3.651 (1)	3.618 (1)	3.583 (1)	3.582 (1)
ESD (%)	3.7	1.6	1.1	2.5

Note: ESD = estimated standard deviation

Figure 1a. Two-dimensional network of $^{2}_{\infty}$[M(ox)(bpy)]. The cross-shaded circles are M (M = Fe, Co, Ni, Zn), open circles are C, solid circle are O, and shaded circles are N.

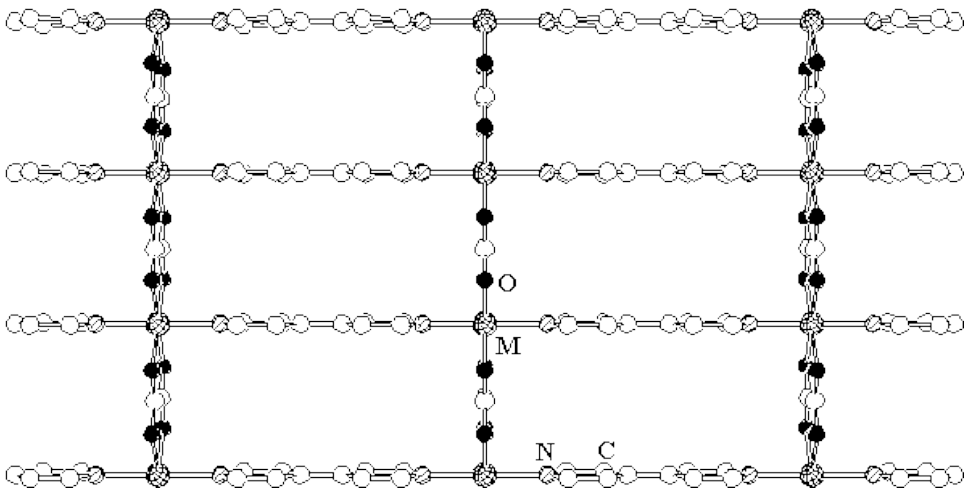

Figure 1b. Perspective view of $^{2}_{\infty}$[M(ox)(bpy)] showing the stacking of 2D nets. The layers are stacked in a staggered fashion along the *b*-axis.

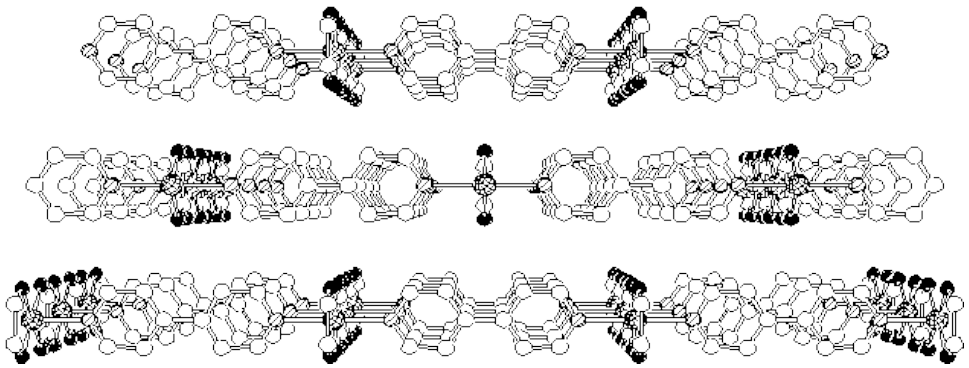

Figure 2a. Two dimensional network of $^{2}_{\infty}$[MCl_2(bpy)]. View along the ***b***-axis showing a single layer.

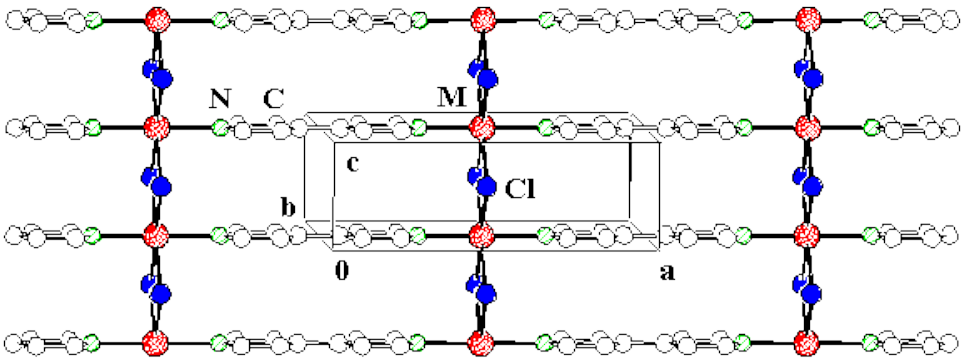

$^{2}_{\infty}$[MCl_2(bpy)](M=Fe, Co, Ni, Co/Ni, Bpy = 4,4'-bipyridine)

Figure 2b. View of $^{2}_{\infty}$[MCl_2(bpy)] along the ***c***-axis showing stacks of layers. The cross-shaded circles are M (M = Fe, Co, Ni, Co/Ni), open circles are C, solid circles are O, and shaded circles are N.

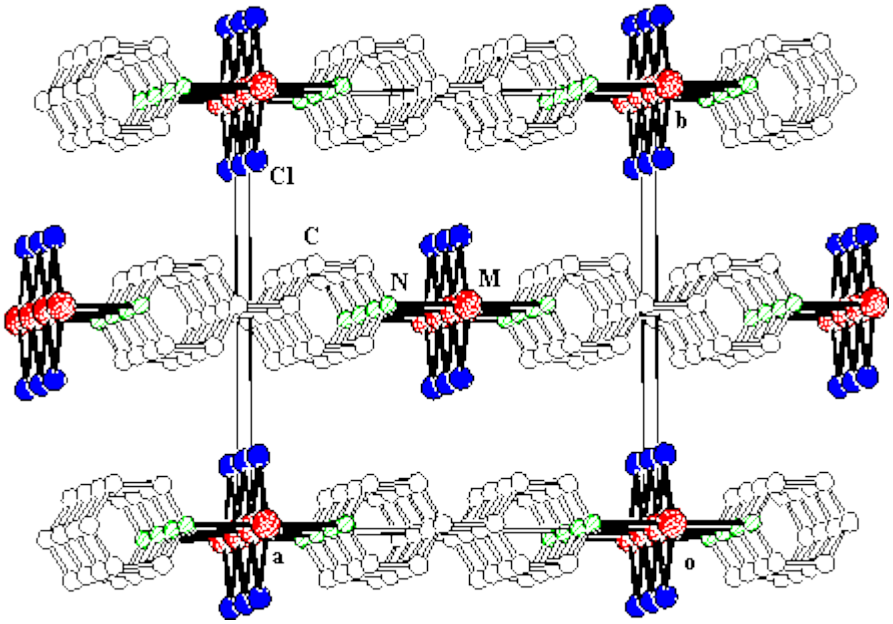

Figure 3. Thermogravimetric analysis (TGA) data showing weight loss of compound **I** (solid line) between 50 and 500°C. The negative of the first derivative (%/°C) is also plotted in each case.

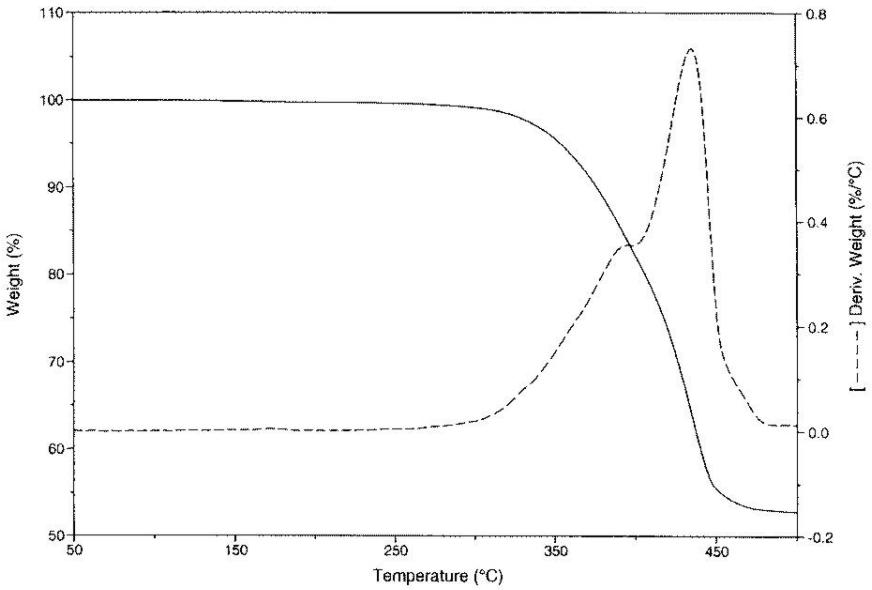

Figure 4. Same as Figure 3, but for compound **II**.

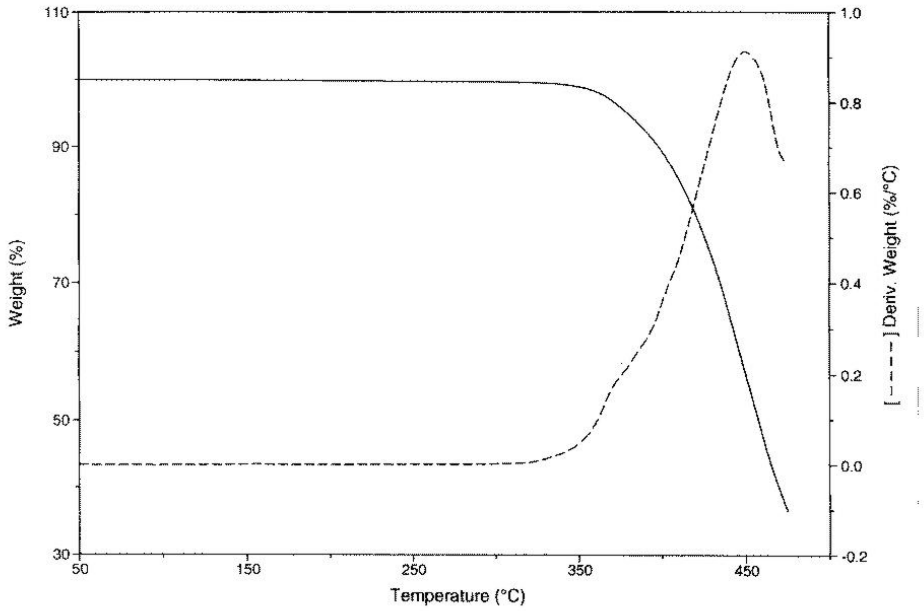

Figure 5. Same as Figure 3 but for compound **III**.

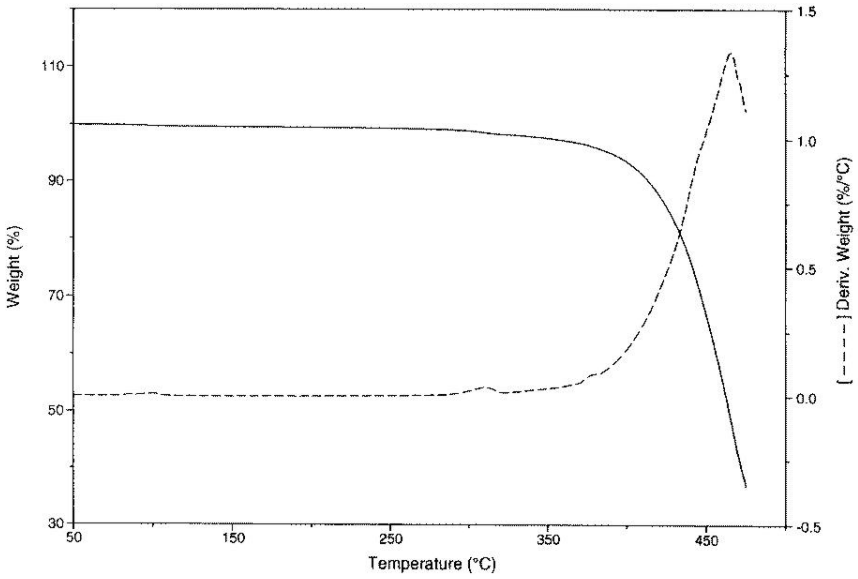

Figure 6. Same as Figure 3 but for compound **IV**.

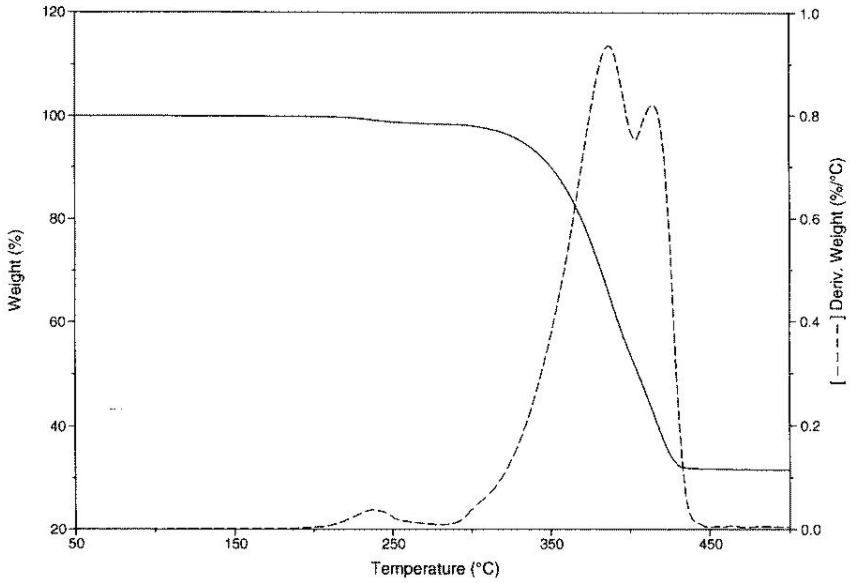

Figure 7. Thermogravimetric analysis (TGA) data showing weight loss of **V** as a function of temperature between 100°C and 800°C. The negative of the first derivative (%/°C) is also plotted as a function of temperature.

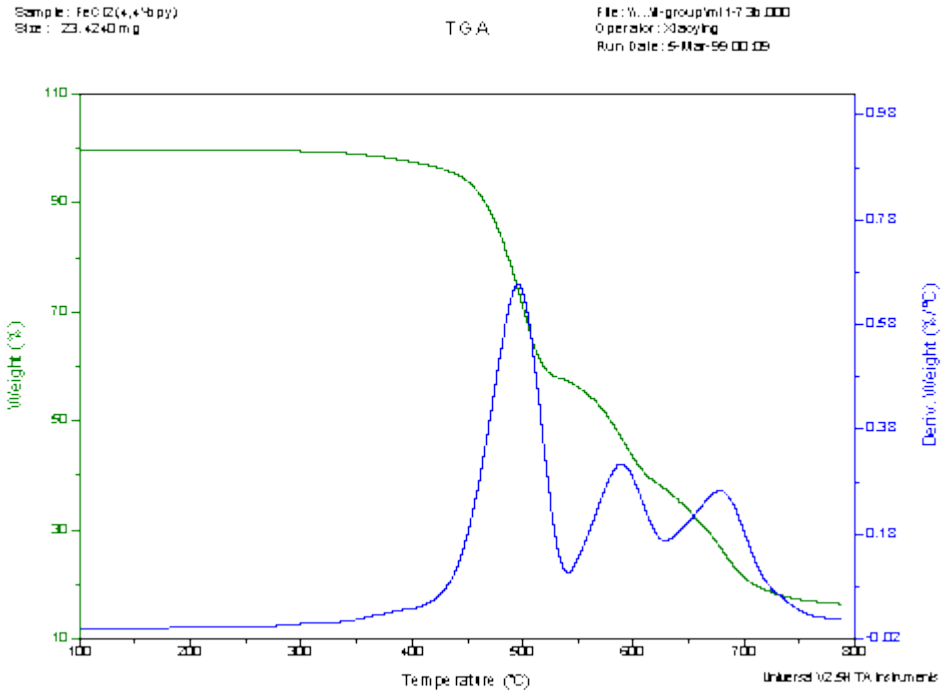

Figure 8. Thermogravimetric analysis (TGA) data showing weight loss of **VI** as a function of temperature between 50°C and 750°C. The negative of the first derivative (%/°C) is also plotted as a function of temperature.

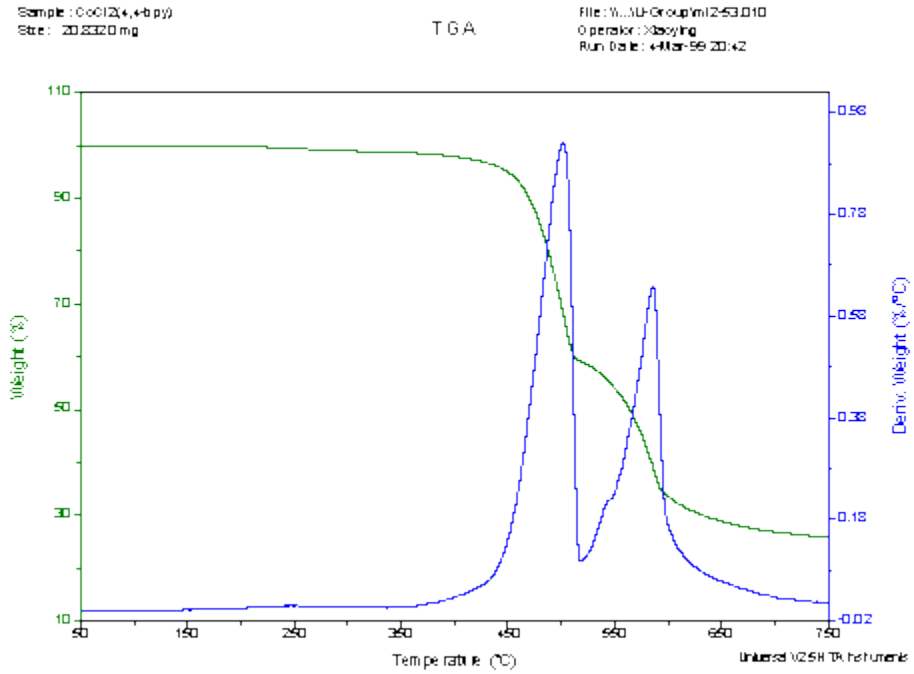

Figures 9 & 10.

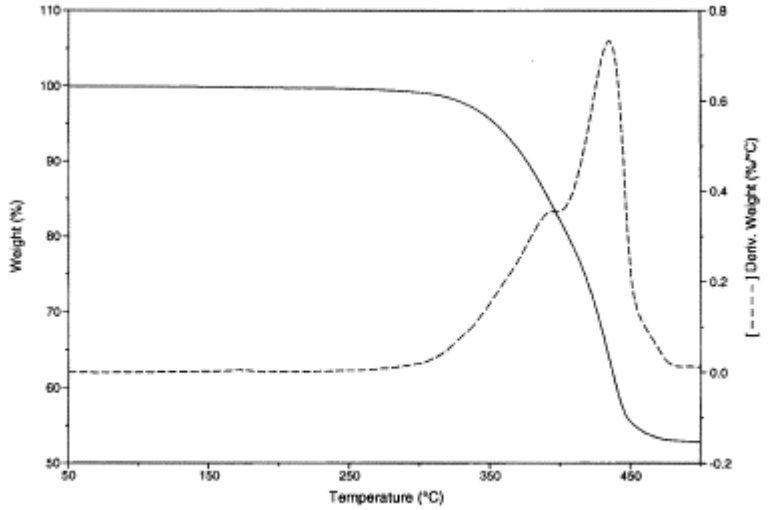

Figure 9. Thermogravimetric analysis (TGA) data showing weight loss of **I** (solid line) between 50 and 500 °C. The negative of the first derivative (%/°C, dashed line) is also plotted as a function of temperature.

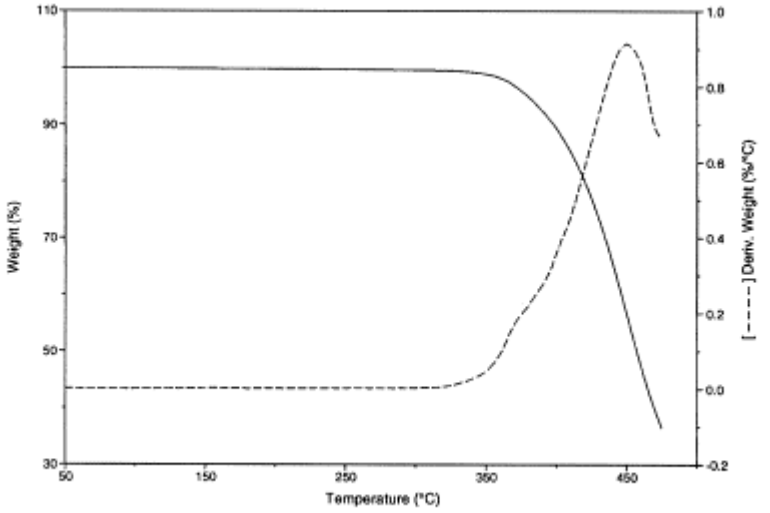

Figure 10. Thermogravimetric analysis (TGA) data showing weight loss of **II** (solid line) between 50 and 500 °C. The negative of the first derivative (%/°C, dashed line) is also plotted as a function of temperature.

Figures 11 & 12.

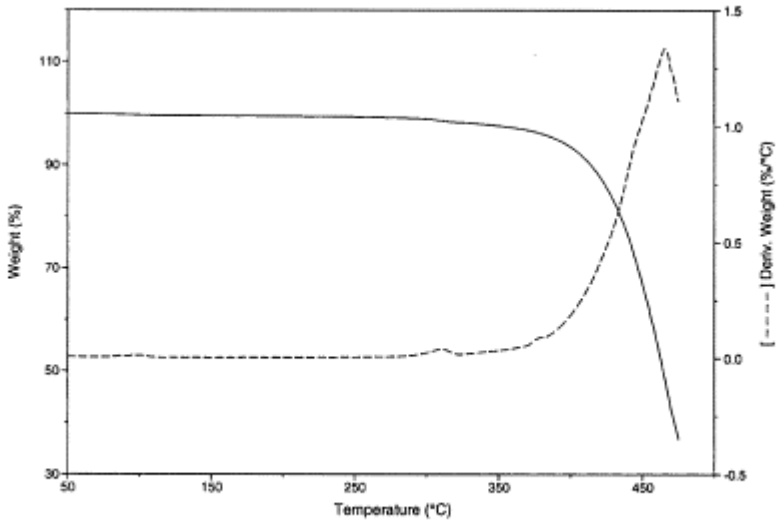

Figure 11. Thermogravimetric analysis (TGA) data showing weight loss of **III** (solid line) between 50 and 500 °C. The negative of the first derivative (%/°C, dashed line) is also plotted as a function of temperature.

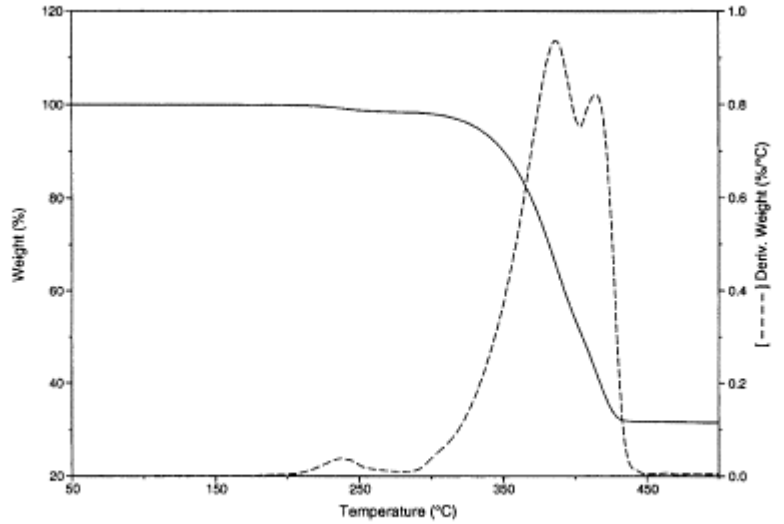

Figure 12. Thermogravimetric analysis (TGA) data showing weight loss of **IV** (solid line) between 50 and 500 °C. The negative of the first derivative (%/°C, dashed line) is also plotted as a function of temperature.